



## Solar Still with an Integrated Conical Condenser

Dan Mugisidi<sup>1,\*</sup>, Berkah Fajar<sup>2</sup>, Syaiful Syaiful<sup>2</sup>, Tony Utomo<sup>2</sup>

<sup>1</sup> Mechanical Engineering, Engineering Faculty, Universitas Muhammadiyah Prof. Dr. HAMKA, Indonesia

<sup>2</sup> Mechanical Engineering, Engineering Faculty, University of Diponegoro, Indonesia

### ARTICLE INFO

#### Article history:

Received 4 August 2022

Received in revised form 5 September 2022

Accepted 2 October 2022

Available online 1 August 2023

#### Keywords:

Desalination; Solar still; Condenser

### ABSTRACT

A solar still requires only two processes: evaporation and condensation. In a solar still, evaporation occurs because of the pressure difference caused by the difference in the temperature of the water and that of the glass cover, while condensation occurs when the water vapour comes into contact with a surface cooler than its dew point. Condensers have been proven to effectively increase the productivity of solar stills. This study aims to compare the efficiency of two developed solar stills with integrated conical condensers to that of a conventional solar still; it also measures the effectiveness of the condenser. Three types of solar stills were used in this study: a conventional solar still (CSS), developed solar still 1 (DSS-1) and developed solar still 2 (DSS-2). All three stills were tested simultaneously. The three solar stills are all made of aluminium with a thickness of 3 mm. The software Ansys Fluent 18.2 was used to analyse the computational fluid dynamics in the stills. The results showed that the efficiency of the CSS, DSS-1 and DSS-2 were 23%, 36.5% and 46.4%, respectively. The freshwater yields of DSS-1 and DSS-2 were, respectively, 1.17 and 1.81 times greater than that of the CSS. These increases in the productivity of DSS-1 and DSS-2 are significantly influenced by the shape of the condenser integrated in these two solar stills; the effectiveness of this condenser was 85.57% and 91.25%, respectively, in DSS-1 and DSS-2. In a simulation, the condenser's effectiveness was 99.85%.

## 1. Introduction

Water is essential to life. Humans, animals and plants cannot survive without water. As the global population increases, water consumption is growing as well. A population increase of 15% will lead to a 40% reduction in available fresh water [1], and, according to UNICEF, half of the world's population could face water scarcity as early as 2025 [2]. In addition to the global threat, the water crisis has become an urgent issue in archipelagic countries such as Indonesia, where coastal villages experience severe water scarcity. There are 12,827 coastal villages throughout Indonesia, and only 66.54% of them have access to clean water [3]. This means that many people must use murky, salty water for their daily needs. The need for clean fresh water is urgent, but fresh water is limited on earth, comprising only 2.8% of available water, while the rest is seawater [4]. Although it contains

\* Corresponding author.

E-mail address: [dan.mugisidi@uhamka.ac.id](mailto:dan.mugisidi@uhamka.ac.id) (Dan Mugisidi)

<https://doi.org/10.37934/cfdl.15.8.122134>

large amounts of salt, seawater offers an important potential water source if it can be efficiently converted into fresh water.

Seawater is converted into fresh water by removing the fluoride,  $\text{CaCO}_3$ , chloride, sodium, sulphate and potassium permanganate ( $\text{KmnO}_4$ ) [5] through a desalination process, making it potable. Desalination is the process of physically removing salt from seawater. One of the most widely used desalination methods is thermal distillation. Distillation uses heat to convert the liquid into water vapour, which then condenses, returning to a liquid state. The water is evaporated slowly to ensure that contaminants in the water are left behind, and the condensed water is uncontaminated; a solar still distils water in this way.

A solar still requires only two processes: evaporation and condensation. Evaporation occurs because of the pressure difference caused by the difference between the temperature of the water and the glass cover; this process is slow [6]. Condensation occurs when the water vapour contacts a surface that is cooler than the dew point; in a still, this occurs randomly on the condenser's surface in a process called dropwise condensation [7]. Adding internal and/or external condensers increases the efficiency of solar stills [8–16], and previous research has explored the use of condensers in solar stills. Expanding the condensing surface increases a solar still's efficiency [17]; for example, in one study, increasing the condensation area by 7.5× increased fresh water production by more than 50% [18]. Furthermore, when a condenser is added to a still, the water in the solar still evaporates in the evaporation chamber, and the water vapour flows towards the low-pressure condenser due to the pressure difference [19]. Continuous, unhindered flow of moisture can significantly increase productivity [20] because uncondensed moisture can decrease system performance and effectiveness [21]. Therefore, including a condenser shaped so that it does not impede the flow of water vapor will improve the solar still's performance. The condenser must have a large inlet so that water vapour can easily flow into it, and, since the condenser's effectiveness is impacted by the amount of water vapour in contact with the condenser wall [22], the vapour must be forced to come into contact with the condenser wall.

Based on these considerations, this study incorporates a conical condenser into a solar still. The opening of the condenser has the same cross section area as the evaporation, but the condenser then narrows so that the water vapour is forced to touch the walls of the condenser. Although the use of condensers in solar stills has been researched in depth, this condenser shape is uncommon and has not been used in a solar still before. To increase the condenser's effectiveness and reduce heat loss, the feed water is also used as the coolant so that the heat released by the water vapour into the condenser is then used to heat the feed water. This study compares the efficiency of a solar still with a conical condenser to that of a conventional solar still (CSS) and measures the effectiveness of the conical condenser on the still's productivity. This study also uses Computational Fluid Dynamics (CFD) simulations to measure the movement of water vapor and the heat transfer that occur in the solar still with an integrated conical condenser.

## **2. Method**

### **2.1 Experimental Setup**

This study compares three types of solar still. Data were collected from all three stills simultaneously to ensure that the input and external conditions were consistent across all three apparatuses. The compared solar stills are a conventional solar still (CSS), a modified solar still with one intake (DSS-1) and a modified solar still with two intakes (DSS-2). DSS-1 and DSS-2 differ only in the number of intakes; their heat absorbers and condenser sizes are the same, as shown in Figure 1.

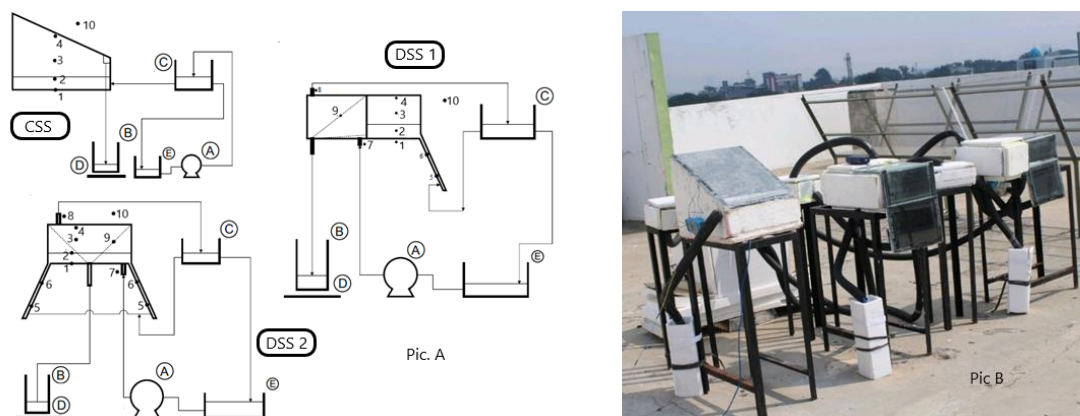


**Fig. 1.** Schematic of CSS, DSS-1 and DSS-2 testing sensors (Pic. A); experimental rig (Pic. B). Numbers 1 through 10 are temperature sensors; 1=Heat absorber plate, 2=Seawater, 3=Evaporation chamber, 4=Inner side of glass cover, 5=Bottom plate sensor, 6=Upper plate sensor, 7= Cooling water inlet, 8=Cooling water outlet, 9=Condenser, 10=Environment; (A)=Circulation pump, (B)=Fresh water reservoir, (C)=Height control, (D)=Scale, (E)=Seawater reservoir.

Figure 1 illustrates the solar stills used in this study. The CSS, which consists of only one chamber, includes a preheater, an evaporation chamber, and a condenser. While the DSS has a condenser integrated with a solar still. The preheater on DSS-1 is only one like single slope solar still and positioned facing east, while the preheaters on DSS-2, like double slope solar still, face east and west. The glass cover of the CSS faces east, while the pump installation regulating water flow is placed on the western side of all three solar stills.

Water flow is generated by three pumps, one serving each solar still. In the CSS, water from the reservoir is pumped into the height control tank. When the water level decreases, the CSS is filled, while water that does not enter the solar tank flows back to the reservoir. The desalinated water flows to a collector placed above the scale. In DSS-1 and DSS-2, the water follows the same flow path. Water from the reservoir is pumped into the condenser, where it serves as a coolant. Afterwards, this water flows back into the reservoir, which drains into the solar still through the bottom of the preheater. Water that does not enter the solar still flows back to the reservoir. In DSS-1 and DSS-2, the desalinated water flows through the bottom of the condenser into the collector above the scales. For this study, all three solar stills were run simultaneously from October 8–10, 2019, from 08:00 to 17:00 (WIB).

In a solar still, evaporation occurs in the evaporation chamber; the bottom of this chamber is lined with iron sand as heat absorber [23, 24]. All three evaporation chambers are 400 mm long and 300 mm wide, with a water height of 10 mm. Thus, the mass/surface area of water on evaporation is 10 kg/m<sup>2</sup>. The lower the water level, the greater the still's productivity. The highest possible water level is 1 cm [25]; when the water is this high, the mass of the water is 2.025 kg. The tools used to retrieve data about the environmental conditions are shown in Table 1.

**Table 1**  
 Tools used in study

No.	Function	Tool	Data
1	Temperature	Thermometer	40–400 °C, 0.09%
2	Solar radiance	Solar meter	0–2000 W/m <sup>2</sup>
3	Wind velocity	Wind meter	0–30 m/s
4	Relative humidity	Hygrometer	10%–99%
5	Weight	Digital scale	0–20 kg ± 0.1

## 2.2 Condenser

Deeper in the condenser, the cross-section becomes smaller and slopes downwards, forcing the water vapor to come into contact with the condenser wall, which has an area of  $104,470.78 \text{ mm}^2$ , or  $0.104 \text{ m}^2$ . As shown in Figure 2 (a) and (b), the slope of the top and bottom of the condenser force the condensed water to flow into the collecting channel. The feed water passes through the space around the condenser, functioning as a coolant and absorbing the heat released by the water vapor during condensation; the average heat transferred from the hot fluid is equal to the average heat received by the cold fluid [7].

$$q_c = \dot{m}_c \cdot c_{pa} \cdot (T_i - T_o) \quad (1)$$

$$q_h = \dot{m}_v \cdot h_{fg} \quad (2)$$

The effectiveness ( $\epsilon$ ) of the condenser is defined as [7]:

$$\epsilon = \frac{q_c}{q_h} \quad (3)$$

where:

- $q_c$  = Heat received by the coolant water in the condenser
- $q_h$  = Heat released by the water vapor during condensation
- $c_{pa}$  = Water heat capacity
- $\dot{m}_c$  = Mass of coolant water
- $\dot{m}_v$  = Mass of water vapor
- $T_i$  = Coolant water inlet temperature
- $T_o$  = Coolant water outlet temperature

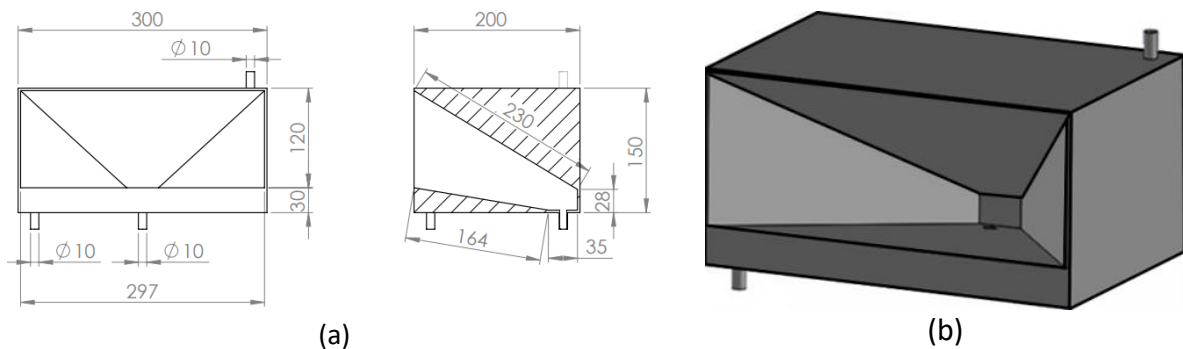


**Fig. 2.** Condenser (a)=Dimensions of condenser, (b)=Conical condenser

The actual heat transferred ( $q_{co}$ ) is the heat received by the coolant water in the condenser, while the maximum heat that can be transferred in the solar still condenser ( $q_{ha}$ ) is the heat released by the water vapour during condensation.

## 2.3 Uncertainty Analyses

An uncertainty analysis aims to measure the variability in output that is caused by input variability [26]. Internal uncertainty ( $u_i$ ) can be estimated using the following equation [27]:

$$u_i = \sqrt{\frac{\sigma_1^2 + \sigma_2^2 + \dots + \sigma_i^2}{N^2}} \quad (4)$$

In this equation,  $u_i$  is the internal uncertainty and  $\sigma_i$  is the standard deviation for each data point, while  $N$  is the number of data points. In this study, uncertainty was measured by calculating the standard deviation between the yield of water produced and solar energy received.

## 2.4 CFD Simulation

Many researchers have conducted simulations using CFD or have used CFD to analyse their findings [28–32]. The CFD simulation in this study was conducted using the software Ansys Fluent 18.2.

Solar radiation passes through the covering glass and is absorbed by the bottom of the basin, heating the water in the basin. Increasing the temperature of the water in the basin increases the pressure on the surface of the water; when the pressure on the surface of the water is higher than that in the evaporation chamber, evaporation occurs.

Grid convergence is very important in multiphase simulations because it affects the accuracy of the simulation [33]; therefore, it is necessary to conduct an independent grid test. The independent grid has converged if the error is less than 1% [34, 35]. In this study, an error of less than 1% was obtained for a 4 mm mesh, as can be seen in Figure 3.

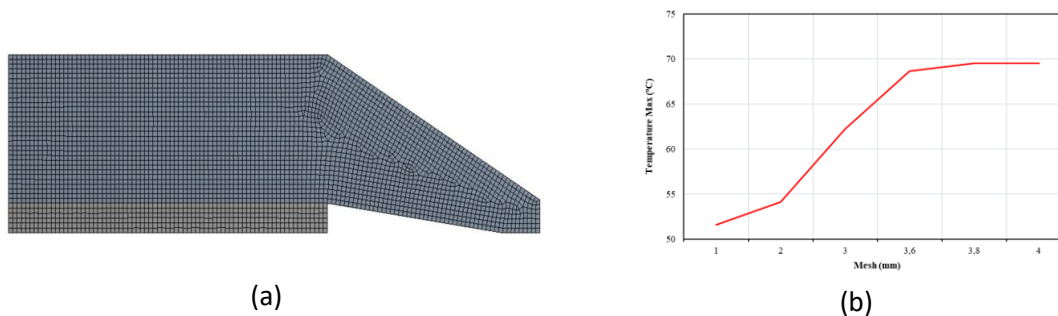


Fig. 3. Mesh (a); Independent grid test (b).

## 3. Results

### 3.1 Uncertainty

The uncertainty for the CSS is 7.8%; for DSS-1, it is 5.4%, and for DSS-2, it is 17.4%. Compared to similar previous studies, the uncertainty in this study is within an expected range, since the uncertainty in other studies ranges from 3.6% [36] to 19% [27]. The research uncertainty in heat transfer should not exceed 25% [7].

### 3.2 Experimental Data

The three solar stills show different temperature trends. Figure 4 shows that, in the CSS, the temperature of the water and the inner glass cover appear to be strongly influenced by incoming solar radiation. The temperatures in DSS-1 and DSS-2 are lower than that in the CSS. However, the production of fresh water in the CSS is influenced by wind speed, which affects the temperature of the glass cover ( $T_{gi}$ ) and, ultimately, the productivity of the still. If  $T_{gi}$  is lower than the dew point, condensation occurs, and the relative humidity in the solar still decreases [37].

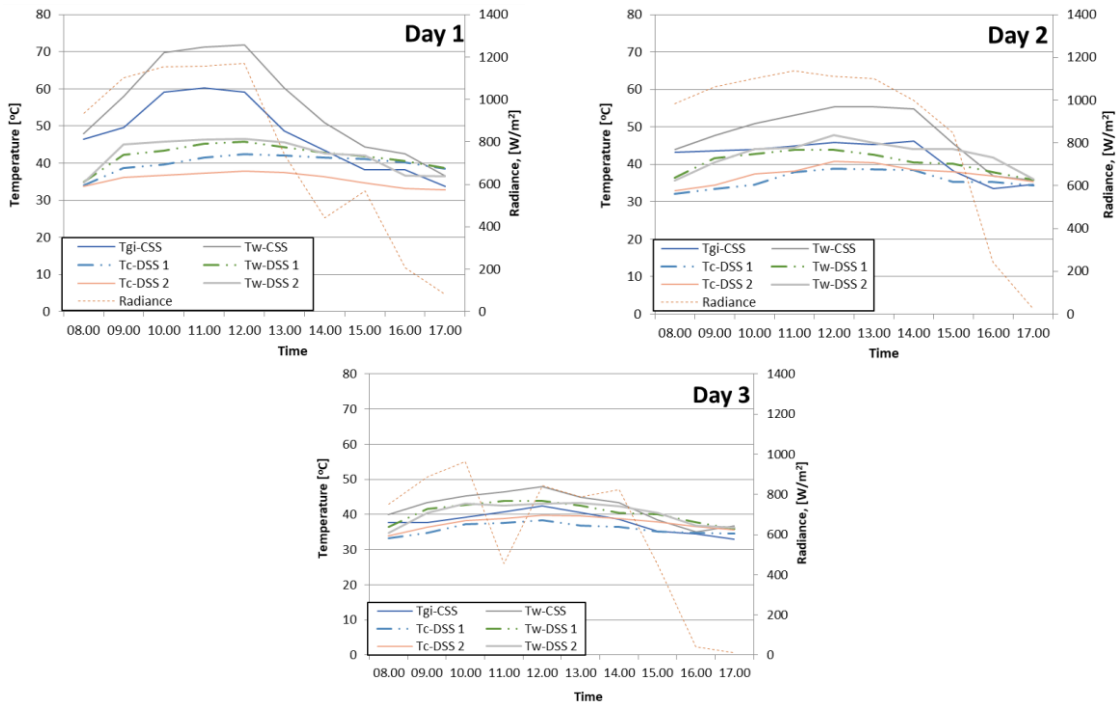


**Fig. 4.** Internal temperatures of the CSS, DSS-1 and DSS-2 on October 8–10, 2019

The difference between the temperature of the water ( $T_w$ ) and that of the inner glass cover ( $T_{gi}$ ) is smaller in the CSS than the difference between  $T_w$  and condenser temperature ( $T_c$ ) in DSS-1 and DSS-2. The pressure difference between the water surface and the condenser surface is the force that drives evaporation since this pressure difference is proportional to the temperature difference [38]. In addition, in DSS-1 and DSS-2, condensation is influenced by the cooling medium. As a result, DSS-1 and DSS-2 yielded more fresh water than the CSS, as shown in Figure 5.

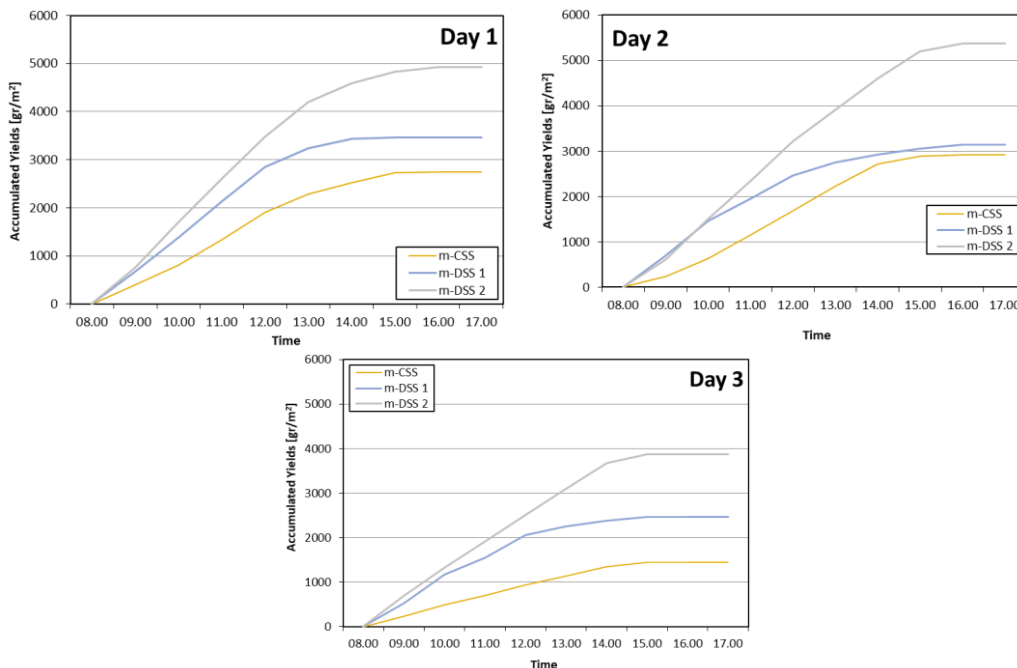


**Fig. 5.** Cumulative yields of the CSS, DSS-1 and DSS-2 for October 8–10, 2019

Figure 6 shows that DSS-1 and DSS-2 produced more fresh water than the CSS with various amounts of solar radiation. However, in DSS-1, water production peaks at 12:00 and then decreases as solar radiation is blocked by the integrated condenser, which prevents the water in the solar still from being heated.

In a solar still, heat transfer occurs naturally. The heat transfer coefficient is calculated using the evaporation heat transfer coefficient, based on the mass of fresh water produced. The assumptions in this calculation are [39]:

- i) There is no water vapour leakage from the solar still.
- ii) The mass of water lost is negligible.
- iii) The water level in the basin is kept constant.

The condensation areas in the CSS and the two DSSs differ; in the CSS, condensation takes place on the inside of the glass cover, while in DSS-1 and DSS-2, condensation takes place in the integrated condenser. Therefore, for the CSS, temperature is measured as  $T_{gi}$  (on the glass cover), while for DSS-1 and DSS-2, it is measured as  $T_c$  (on the condenser). The Nusselt number ( $Nu$ ) is obtained by first calculating the evaporation heat transfer coefficient ( $h_{ew}$ ) and the convection heat transfer coefficient ( $h_{cw}$ ) based on the mass of the water produced [40].

A power regression is used to determine the values of  $C$  and  $n$  [41]. For the CSS, the average  $C = 0.92$  and the average  $n = 0.05$ . For DSS-1, the average  $C = 0.92$  and the average  $n = 0.09$ , and for DSS-2, the average  $C = 0.91$  and the average  $n = 0.15$

After  $C$  and  $n$  have been calculated, the Nusselt number can be obtained using the Nusselt-Rayleigh equation, which is also used to obtain the convection heat transfer coefficient [42]:

$$Nu = \frac{h_c d_f}{k_f} = C \cdot (G_r \cdot P_r)^n \tag{5}$$

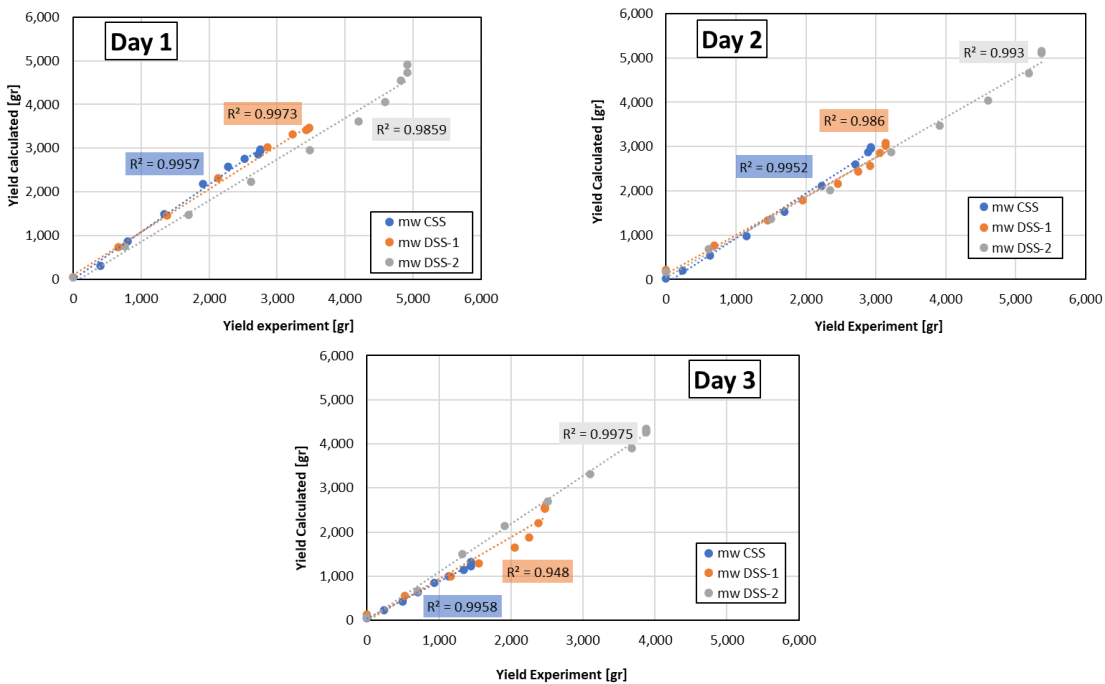


Fig. 6. Cumulative yields of the CSS, DSS-1 and DSS-2, October 8–10, 2019

Using the results of these calculations, the yield of fresh water can be predicted. The coefficient determination ( $R^2$ ) of the experimental water mass with these calculations ranges from 0.9952 to 0.9958 for the CSS. For DSS-1,  $R^2$  ranges from 0.9480 to 0.9973, and for DSS-2,  $R^2$  ranges from 0.993 to 0.9975. This indicates a high correlation amongst the water masses for all three types of solar still [43]. These results can be used to predict the yields of the solar stills. Furthermore, the efficiency of each solar still can be calculated.

The thermal efficiency of a solar still depends on the daily yield accumulation, the daily solar intensity, the latent heat of vaporisation and the surface area of the condensation area. Mathematically, it is expressed by the following equation [44]:

$$\eta = \frac{\sum m_w \cdot h_{fg}}{\sum I \cdot A \cdot 3600} \quad (6)$$

The solar stills with integrated condensers are more efficient than the CSS. The solar still with the integrated DSS-2 condenser reached the highest efficiency, 47.3%; this still's average efficiency over three days was 46.5%. DSS-2 also has high efficiency compared to previously reported stills with integrated or separate condensers [12, 45–53]. This high efficiency cannot be separated from the shape of the condenser, which narrows towards the exit. This shape forces the water vapour to come into contact with the condenser wall, causing condensation to occur. A CFD simulation is used to explain the phenomena that occur in the solar still and condenser. The experimental data in this study differed from the CFD simulation by less than 6.63%. The simulations for temperature distribution and the velocity vector for DSS-2 are shown in Figure 7.

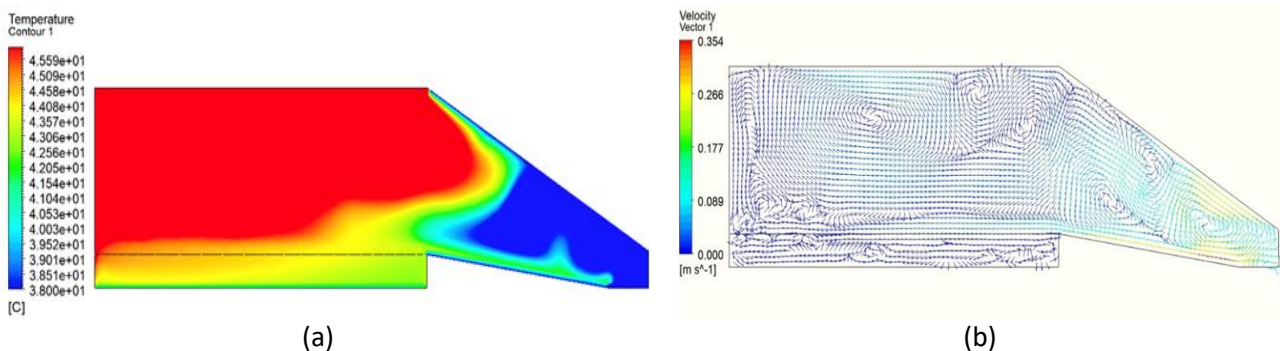


**Fig. 7.** Temperature distribution (a) and velocity vector (b) for DSS-2 condenser.

The simulated temperature distribution in the DSS-2 condenser, shown in Figure 7 (a), shows that the highest temperature in the solar still is located in the evaporation area above the seawater. These simulation results align with the experimental data in this study and also with the findings of previous similar studies [54–58]. Condensation begins above the surface of the water and extends to the inner glass cover. In DSS-2, the glass cover comprises two layers of glass separated by an air gap of 3 mm. The water vapour formed during evaporation accumulates in the evaporation area. Since water vapour can absorb heat, the incoming solar heat causes the pressure and temperature of water vapour in the evaporation area to rise. In a CSS, water usually condenses on the inside of the glass cover. However, this does not occur with the double glass cover because the heat inside still moves slowly outward, as the wind does not cool the inner glass. This maintains the temperature of the inner layer of glass above the condensation temperature, preventing condensation [53]. Since there is no condensation, the water vapour pressure in the evaporation area increases. Although water vapour tends to move upwards, the pressure difference between the evaporation area and the environment makes the water vapour move towards the condenser outlet, as shown in Figure 7 (b).



Figure 7 (b) shows the movement of the water vapour, which is caused by buoyancy and pressure differences. The vapor moves from the evaporation area to the condenser without any change in velocity. Thus, the vapor flows easily into the condenser, without any disturbance. The vapour changes velocity as the condenser narrows; the flow of water vapor then forms a rotating stream or vortex which moves towards the outlet. Meanwhile, the water vapour above the surface of the water moves directly towards the condenser because the pressure in that region is higher than the pressure in the condenser. This vapour accelerates as it approaches the condensate outlet. Since the vapour velocity increases inside the condenser as the condenser's cross-sectional area decreases, more vapour comes into contact with the condenser wall and condenses.

Condensation occurs at the condenser wall because the moving vapour comes into contact with the condenser wall. However, the simulation shows that not all water vapour contacts the condenser wall; some vapour exits directly through the condensate outlet. Therefore, the condenser's effectiveness is calculated using the mass of water produced and the heat received by the cooling water in the condenser. The inlet and outlet temperature are shown in Table 2; effectiveness is calculated using Eq. (1) to Eq. (3). The results of these calculations are shown in Table 3.

**Table 2**  
 Inlet (Ti) and outlet (To) temperature of condenser in DSS-1 and DSS-2

Jam	8 Oct 2019				9 Oct 2019				10 Oct 2019			
	Tc DSS-1		Tc DSS-2		Tc DSS-1		Tc DSS-2		Tc DSS-1		Tc DSS-2	
	In	Out	In	Out	In	Out	In	Out	In	Out	In	Out
8	30.4	30.4	30.2	30.3	30.2	30.4	30.2	30.3	30.2	30.6	30.3	30.8
9	30.3	32.0	30.3	32.3	30.4	31.9	30.3	31.7	30.5	31.3	30.3	31.9
10	30.4	32.4	30.4	32.5	30.5	32.2	30.4	32.3	30.5	31.8	30.6	32.8
11	30.4	32.8	30.4	32.6	30.5	31.8	30.7	32.6	30.5	31.4	30.6	32.6
12	30.5	32.7	30.4	32.5	30.4	31.5	30.8	33.3	30.5	31.5	30.6	32.3
13	30.6	31.5	30.5	32.3	30.3	31.1	30.8	32.6	30.5	31.2	30.4	32.2
14	30.5	30.8	30.5	31.8	30.5	30.9	30.9	32.6	30.3	31.3	30.4	32.1
15	30.4	30.5	30.4	31.8	30.3	30.9	30.7	32.6	30.3	31.2	30.4	32.1
16	30.3	30.3	30.4	31.0	30.2	30.5	30.6	31.9	30.3	30.3	30.2	30.3
17	30.3	30.3	30.4	30.6	30.0	29.8	30.3	30.5	30.3	30.3	30.1	30.0

**Table 3**  
 Condenser effectiveness in the CSS, DSS-1 and DSS-2

	CSS	DSS-1	DSS-2
8 Oct 2019	10.77%	88.18%	91.09%
9 Oct 2019	21.19%	84.24%	92.46%
10 Oct 2019	27.76%	84.29%	90.20%
average	19.91%	85.57%	91.25%

Table 2 shows the effectiveness of the condensers. The effectiveness of the CSS condenser, which is also the glass cover of the solar still, is only around 20%. The calculation includes a temperature difference because even when the difference between the water temperature and the inside of the glass reaches 12.6 °C, the water vapour does not always condense on the top glass cover. Condensation on the glass cover is strongly influenced by wind speed, which is an external factor. The wind does not affect the DSS-1 and DSS-2 because these solar stills have double-layer glass covers. This ensures that the water vapour formed in the evaporation chamber does not condense and instead flows into the condenser. Moreover, a large amount of vapour generated from the evaporation process in the solar still contacts the condenser wall. The effectiveness of DSS-1 is

85.57%, and that of DSS-2 is 91.55%. The width of the condenser impacts its effectiveness [59]. In DSS-1 and DSS-2, the chute cross-section decreases towards the outlet, forcing more water vapour to touch the walls of the condenser. Experimental and model results show that the conical condenser used in DSS-1 and DSS-2 is effective.

#### 4. Conclusions

This study has obtained fresh water by evaporating seawater and recondensing it using three types of solar still. The results show that DSS-1 and DSS-2 were 1.76 times and 2.24 times more productive than the CSS, respectively. DSS-2 is also more efficient than stills described in previous studies; its efficiency reached 47.3%, while the efficiency of the CSS and DSS-1 were 23% and 36.5%, respectively. The increased productivity of DSS-1 and DSS-2 is strongly influenced by the shape of the condenser integrated into these two solar stills. The increased productivity of DSS-1 and DSS-2 is also strongly influenced by the shape of the integrated condenser. The effectiveness of the integrated conical condenser reached 85.57% and 91.25% in DSS-1 and DSS-2, respectively; in the simulation, it reached 99.85%. Therefore, a conical condenser is more effective than a conventional condenser, and its use in solar stills should be developed further.

#### Acknowledgement

This research was supported by the Office of Research and Development and UPPI at Universitas Muhammadiyah Prof. Dr. Hamka.

#### References

- [1] Schewe, Jacob, Jens Heinke, Dieter Gerten, Ingjerd Haddeland, Nigel W. Arnell, Douglas B. Clark, Rutger Dankers et al. "Multimodel assessment of water scarcity under climate change." *Proceedings of the National Academy of Sciences* 111, no. 9 (2014): 3245-3250. <https://doi.org/10.1073/pnas.1222460110>
- [2] UNICEF. "Water Scarcity." Accessed August 5, 2022. <https://www.unicef.org/wash/water-scarcity>.
- [3] LIPI, "Indonesia Negeri Tropis, Tapi Krisis Air Bersih di Kawasan Pesisir Terjadi? [Indonesia is a Tropical Country, But Has a Clean Water Crisis Happened in Coastal Areas?]," Mar. 23, 2018. Accessed August 5, 2022 <http://lipi.go.id/lipimedia/Indonesia-Negeri-Tropis-Tapi-Krisis-Air-Bersih-di-Kawasan-Pesisir-Terjadi/20218>
- [4] Belessiotis, Vassilis, Soteris Kalogirou, and Emmy Delyannis. *Thermal solar desalination: Methods and systems*. Elsevier, 2016.
- [5] Mugisidi, Dan, and Okatrina Heriyani. "Sea water characterization at ujung kulon coastal depth as raw water source for desalination and potential energy." In *E3S Web of Conferences*, vol. 31, p. 02005. EDP Sciences, 2018. <https://doi.org/10.1051/e3sconf/20183102005>
- [6] Mahian, Omid, Ali Kianifar, Saeed Zeinali Heris, Dongsheng Wen, Ahmet Z. Sahin, and Somchai Wongwises. "Nanofluids effects on the evaporation rate in a solar still equipped with a heat exchanger." *Nano energy* 36 (2017): 134-155. <https://doi.org/10.1016/j.nanoen.2017.04.025>
- [7] Holman, J. P. "Heat Transfer-Natural Convection Systems, Chap. 7." *McGraw-Hill, New York* (2010): 327-378.
- [8] Jourabchi, Seyed Amirmostafa, Suyin Gan, and Hoon Kiat Ng. "Pyrolysis of *Jatropha curcas* pressed cake for bio-oil production in a fixed-bed system." *Energy Conversion and Management* 78 (2014): 518-526. <https://doi.org/10.1016/j.enconman.2013.11.005>
- [9] Essa, F. A., Mohamed Abd Elaziz, and Ammar H. Elsheikh. "An enhanced productivity prediction model of active solar still using artificial neural network and Harris Hawks optimizer." *Applied Thermal Engineering* 170 (2020): 115020. <https://doi.org/10.1016/j.applthermaleng.2020.115020>
- [10] El-Samadony, Y. A. F., A. S. Abdullah, and Z. M. Omara. "Experimental study of stepped solar still integrated with reflectors and external condenser." *Experimental heat transfer* 28, no. 4 (2015): 392-404. <https://doi.org/10.1080/08916152.2014.890964>
- [11] Al-Hamadani, Ali AF, and S. K. Shukla. "Performance of single slope solar still with solar protected condenser." *Distributed Generation & Alternative Energy Journal* 28, no. 2 (2013): 6-28. <https://doi.org/10.1080/21563306.2013.10677548>

- [12] Sivaram, P. M., S. Dinesh Kumar, M. Premalatha, T. Sivasankar, and A. Arunagiri. "Experimental and numerical study of stepped solar still integrated with a passive external condenser and its application." *Environment, Development and Sustainability* 23 (2021): 2143-2171. <https://doi.org/10.1007/s10668-020-00667-4>
- [13] Ahmed, Husham M., Ghaleb Ibrahim, and Geraldo C. Talisic. "Thermal performance of a conventional solar still with a built-in passive condenser: experimental studies." *J. Adv. Sci. Eng. Res* 7, no. 3 (2017): 1-12.
- [14] Belhadj, Mohamed Mustapha, Hamza Bouguettaia, Yacine Marif, and Moussa Zerrouki. "Numerical study of a double-slope solar still coupled with capillary film condenser in south Algeria." *Energy Conversion and Management* 94 (2015): 245-252. <https://doi.org/10.1016/j.enconman.2015.01.069>
- [15] Tiwari, G. N., A. Kupfermann, and Shruti Aggarwal. "A new design for a double-condensing chamber solar still." *Desalination* 114, no. 2 (1997): 153-164. [https://doi.org/10.1016/S0011-9164\(98\)00007-1](https://doi.org/10.1016/S0011-9164(98)00007-1)
- [16] El-Bahi, A., and D. Inan. "Analysis of a parallel double glass solar still with separate condenser." *Renewable energy* 17, no. 4 (1999): 509-521. [https://doi.org/10.1016/S0960-1481\(98\)00768-X](https://doi.org/10.1016/S0960-1481(98)00768-X)
- [17] Xiong, Jianyin, Guo Xie, and Hongfei Zheng. "Experimental and numerical study on a new multi-effect solar still with enhanced condensation surface." *Energy conversion and management* 73 (2013): 176-185. <https://doi.org/10.1016/j.enconman.2013.04.024>
- [18] Bhardwaj, R., M. V. Ten Kortenaar, and R. F. Mudde. "Maximized production of water by increasing area of condensation surface for solar distillation." *Applied energy* 154 (2015): 480-490. <https://doi.org/10.1016/j.apenergy.2015.05.060>
- [19] Fath, Hassan ES, and Samy M. Elsherbiny. "Effect of adding a passive condenser on solar still performance." *Energy Conversion and Management* 34, no. 1 (1993): 63-72. [https://doi.org/10.1016/0196-8904\(93\)90008-X](https://doi.org/10.1016/0196-8904(93)90008-X)
- [20] Ho-Ming, Yeh, Ten Lin-Wen, and Chen Lie-Chaing. "Basin-type solar distillers with operating pressure reduced for improved performance." *Energy* 10, no. 6 (1985): 683-688. [https://doi.org/10.1016/0360-5442\(85\)90101-X](https://doi.org/10.1016/0360-5442(85)90101-X)
- [21] Charef, Adil, Monssif Najim, and Hicham Meftah. "Liquid film condensation from water vapour flowing downward along a vertical tube." *Desalination* 409 (2017): 21-31. <https://doi.org/10.1016/j.desal.2017.01.018>
- [22] Refalo, Paul, Robert Ghirlando, and Stephen Abela. "The use of a solar chimney and condensers to enhance the productivity of a solar still." *Desalination and Water Treatment* 57, no. 48-49 (2016): 23024-23037. <https://doi.org/10.1080/19443994.2015.1106096>
- [23] Mugisidi, Dan, Berkah Fajar, Syaiful Syaiful, Tony Utomo, Oktarina Heriyani, Delvis Agusman, and Regita Regita. "Iron Sand as a Heat Absorber to Enhance Performance of a Single-Basin Solar Still." *Journal of Advanced Research in Fluid Mechanics and Thermal Sciences* 70, no. 1 (2020): 125-135. <https://doi.org/10.37934/arfmts.70.1.125135>
- [24] Mugisidi, Dan, Berkah Fajar, and Tony Utomo. "The effect of water surface level in sensible heat material on yield of Single Basin solar still: experimental study." In *Journal of Physics: Conference Series*, vol. 1373, no. 1, p. 012014. IOP Publishing, 2019. <https://doi.org/10.1088/1742-6596/1373/1/012014>
- [25] Elango, T., and K. Kalidasa Murugavel. "The effect of the water depth on the productivity for single and double basin double slope glass solar stills." *Desalination* 359 (2015): 82-91. <https://doi.org/10.1016/j.desal.2014.12.036>
- [26] Geffray, C., A. Gerschenfeld, Pavel Kudinov, Ignas Mickus, Marti Jeltsov, Kaspar Kööp, Dmitry Grishchenko, and D. Pointer. "Verification and validation and uncertainty quantification." In *Thermal Hydraulics Aspects of Liquid Metal Cooled Nuclear Reactors*, pp. 383-405. Woodhead Publishing, 2019. <https://doi.org/10.1016/B978-0-08-101980-1.00008-9>
- [27] Kumar, Sanjay, and G. N. Tiwari. "Estimation of convective mass transfer in solar distillation systems." *Solar energy* 57, no. 6 (1996): 459-464. [https://doi.org/10.1016/S0038-092X\(96\)00122-3](https://doi.org/10.1016/S0038-092X(96)00122-3)
- [28] Nadgire, Anand R., Shivprakash B. Barve, and Prachi K. Ithape. "Experimental investigation and performance analysis of double-basin solar still using CFD techniques." *Journal of The Institution of Engineers (India): Series C* 101 (2020): 531-539. <https://doi.org/10.1007/s40032-020-00561-y>
- [29] Khare, Vaibhav Rai, Abhay Pratap Singh, Hemant Kumar, and Rahul Khatri. "Modelling and performance enhancement of single slope solar still using CFD." *Energy Procedia* 109 (2017): 447-455. <https://doi.org/10.1016/j.egypro.2017.03.064>
- [30] Mahmoud, S., Asko Ellman, Ahmed Hegazy, and Tarek Ghonim. "Experimental Analysis and CFD Modeling for Conventional Basin-Type Solar Still."
- [31] Yan, Tiantong, Guo Xie, Hongtao Liu, Zhanglin Wu, and Licheng Sun. "CFD investigation of vapor transportation in a tubular solar still operating under vacuum." *International Journal of Heat and Mass Transfer* 156 (2020): 119917. <https://doi.org/10.1016/j.ijheatmasstransfer.2020.119917>
- [32] Mugisidi, Dan, Oktarina Heriyani, Pancatativa Hesti Gunawan, and Dwi Apriani. "Performance Improvement of a Forced Draught Cooling Tower Using a Vortex Generator." *CFD Letters* 13, no. 1 (2021): 45-57. <https://doi.org/10.37934/cfdl.13.1.4557>

- [33] Hamad, A., Syed Mohammed Aminuddin Aftab, and Kamarul Arifin Ahmad. "Reducing flow separation in T-junction pipe using vortex generator: CFD study." *Journal of Advanced Research in Fluid Mechanics and Thermal Sciences* 44, no. 1 (2018): 36-46.
- [34] Shoeibi, Shahin, Nader Rahbar, Ahad Abedini Esfahlani, and Hadi Kargarsharifabad. "Energy matrices, exergoeconomic and enviroeconomic analysis of air-cooled and water-cooled solar still: Experimental investigation and numerical simulation." *Renewable Energy* 171 (2021): 227-244. <https://doi.org/10.1016/j.renene.2021.02.081>
- [35] Gnanavel, C., R. Saravanan, and M. Chandrasekaran. "CFD analysis of solar still with PCM." *Materials Today: Proceedings* 37 (2021): 694-700. <https://doi.org/10.1016/j.matpr.2020.05.638>
- [36] Halima, Hanen Ben, Nader Frikha, and Slimane Gabsi. "Experimental study of a bubble basin intended for water desalination system." *Desalination* 406 (2017): 10-15. <https://doi.org/10.1016/j.desal.2016.08.003>
- [37] Deshmukh, H. S., and S. B. Thombre. "Solar distillation with single basin solar still using sensible heat storage materials." *Desalination* 410 (2017): 91-98. <https://doi.org/10.1016/j.desal.2017.01.030>
- [38] Abu-Hijleh, Bassam AK. "Enhanced solar still performance using water film cooling of the glass cover." *desalination* 107, no. 3 (1996): 235-244. [https://doi.org/10.1016/S0011-9164\(96\)00165-8](https://doi.org/10.1016/S0011-9164(96)00165-8)
- [39] Elango, C., N. Gunasekaran, and K. Sampathkumar. "Thermal models of solar still—A comprehensive review." *Renewable and Sustainable Energy Reviews* 47 (2015): 856-911. <https://doi.org/10.1016/j.rser.2015.03.054>
- [40] Dan Mugisidi, Dan Mugisidi, Abdul Rahman Abdul Rahman, Oktarina Heriyani Oktarina Heriyani, and Pancatstva Hesti Gunawan Pancatstva Hesti Gunawan. "Determination of the convective heat transfer constant (c and n) in a solar still." *Jurnal Ilmiah Sains dan Teknologi* 11, no. 1 (2021): 1-12. <https://doi.org/10.22146/teknosains.50908>
- [41] Mohamed, A. F., A. A. Hegazi, G. I. Sultan, and Emad MS El-Said. "Augmented heat and mass transfer effect on performance of a solar still using porous absorber: experimental investigation and exergetic analysis." *Applied Thermal Engineering* 150 (2019): 1206-1215. <https://doi.org/10.1016/j.applthermaleng.2019.01.070>
- [42] Tsilingiris, Panayotis T. "Parameters affecting the accuracy of Dunkle's model of mass transfer phenomenon at elevated temperatures." *Applied Thermal Engineering* 75 (2015): 203-212. <https://doi.org/10.1016/j.applthermaleng.2014.09.010>
- [43] Pertiwi, Monica Apriliana, and Sutomo Kahar. "Analisis Korelasi Suhu Permukaan Laut Terhadap Curah Hujan Dengan Metode Penginderaan Jauh Tahun 2012-2013 (Studi Kasus: Kota Semarang)." *Jurnal Geodesi Undip* 4, no. 1 (2015): 61-71.
- [44] Manokar, A. Muthu, Yazan Taamneh, D. Prince Winston, P. Vijayabalan, D. Balaji, Ravishankar Sathyamurthy, S. Padmanaba Sundar, and D. Mageshbabu. "Effect of water depth and insulation on the productivity of an acrylic pyramid solar still—An experimental study." *Groundwater for Sustainable Development* 10 (2020): 100319. <https://doi.org/10.1016/j.gsd.2019.100319>
- [45] Hassan, Hamdy, Mohamed S. Yousef, Mohamed Fathy, and M. Salem Ahmed. "Impact of condenser heat transfer on energy and exergy performance of active single slope solar still under hot climate conditions." *Solar Energy* 204 (2020): 79-89. <https://doi.org/10.1016/j.solener.2020.04.026>
- [46] Amarloo, A., and M. B. Shafii. "Enhanced solar still condensation by using a radiative cooling system and phase change material." *Desalination* 467 (2019): 43-50. <https://doi.org/10.1016/j.desal.2019.05.017>
- [47] Ibrahim, Ghaleb, and Husham M. Ahmed. "Theoretical and Experimental Analysis of Solar Still with Integrated Built-in Condenser." *International Journal of Engineering and Technology(UAE)* 7, no. 4.15 (October 7, 2018): 327. <https://doi.org/10.14419/ijet.v7i4.15.23022>
- [48] Tuly, S. S., M. S. Rahman, M. R. I. Sarker, and R. A. Beg. "Combined influence of fin, phase change material, wick, and external condenser on the thermal performance of a double slope solar still." *Journal of Cleaner Production* 287 (2021): 125458. <https://doi.org/10.1016/j.jclepro.2020.125458>
- [49] Hassan, Hamdy, M. Salem Ahmed, Mohamed Fathy, and Mohamed S. Yousef. "Impact of salty water medium and condenser on the performance of single acting solar still incorporated with parabolic trough collector." *Desalination* 480 (2020): 114324. <https://doi.org/10.1016/j.desal.2020.114324>
- [50] Fath, Hassan ES, Samy Elsherbiny, and Ahmad Ghazy. "A naturally circulated humidifying/dehumidifying solar still with a built-in passive condenser." *Desalination* 169, no. 2 (2004): 129-149. [https://doi.org/10.1016/S0011-9164\(04\)00521-1](https://doi.org/10.1016/S0011-9164(04)00521-1)
- [51] Ahmed, Husham M. "Experimental investigations of solar stills connected to external passive condensers." *Journal of Advanced Science and Engineering Research* 2, no. 1 (2012): 1-11.
- [52] Kabeel, A. E., Z. M. Omara, and F. A. Essa. "Numerical investigation of modified solar still using nanofluids and external condenser." *Journal of the Taiwan Institute of Chemical Engineers* 75 (2017): 77-86. <https://doi.org/10.1016/j.jtice.2017.01.017>

- [53] Rahmani, Ahmed, Abdelouahab Boutriaa, and Amar Hadeif. "An experimental approach to improve the basin type solar still using an integrated natural circulation loop." *Energy conversion and management* 93 (2015): 298-308. <https://doi.org/10.1016/j.enconman.2015.01.026>
- [54] Hansen, R. Samuel, C. Surya Narayanan, and K. Kalidasa Murugavel. "Performance analysis on inclined solar still with different new wick materials and wire mesh." *Desalination* 358 (2015): 1-8. <https://doi.org/10.1016/j.desal.2014.12.006>
- [55] Kumar, R. Arun, G. Esakkimuthu, and K. Kalidasa Murugavel. "Performance enhancement of a single basin single slope solar still using agitation effect and external condenser." *Desalination* 399 (2016): 198-202. <https://doi.org/10.1016/j.desal.2016.09.006>
- [56] Reddy, K. S., and H. Sharon. "Active multi-effect vertical solar still: Mathematical modeling, performance investigation and enviro-economic analyses." *Desalination* 395 (2016): 99-120. <https://doi.org/10.1016/j.desal.2016.05.027>
- [57] Ouar, ML Ali, M. H. Sellami, S. E. Meddour, R. Touahir, S. Guemari, and K. Loudiyi. "Experimental yield analysis of groundwater solar desalination system using absorbent materials." *Groundwater for Sustainable Development* 5 (2017): 261-267. <https://doi.org/10.1016/j.gsd.2017.08.001>
- [58] Morad, M. M., Hend AM El-Maghawry, and Kamal I. Wasfy. "A developed solar-powered desalination system for enhancing fresh water productivity." *Solar Energy* 146 (2017): 20-29. <https://doi.org/10.1016/j.solener.2017.02.002>
- [59] Rahmani, Ahmed, and Abdelouahab Boutriaa. "Numerical and experimental study of a passive solar still integrated with an external condenser." *international journal of hydrogen energy* 42, no. 48 (2017): 29047-29055. <https://doi.org/10.1016/j.ijhydene.2017.07.242>